


# NCAPD2 promotes breast cancer progression through E2F1 transcriptional regulation of CDK1

Jinsong He<sup>1</sup>  | Rui Gao<sup>1</sup> | Jianbo Yang<sup>2,3</sup> | Feng Li<sup>1</sup> | Yang Fu<sup>1</sup> | Junwei Cui<sup>1</sup> | Xiaoling Liu<sup>1</sup> | Kanghua Huang<sup>1</sup> | Qiuyi Guo<sup>1</sup> | Zihan Zhou<sup>1</sup> | Wei Wei<sup>1</sup>

<sup>1</sup>Department of Breast Surgery, Peking University Shenzhen Hospital, Shenzhen, Guangdong, China

<sup>2</sup>Department of The Cancer Center, Fujian Medical University Union Hospital, Fuzhou, Fujian, China

<sup>3</sup>Department of Otolaryngology, The Immunotherapy Research Laboratory, University of Minnesota, Minneapolis, Minnesota, USA

## Correspondence

Jinsong He, Department of Breast Surgery, Peking University Shenzhen Hospital, 1120 Lianhua Road, Futian District, Shenzhen, Guangdong 518036, China.  
Email: [hjssums@sohu.com](mailto:hjssums@sohu.com)

## Funding information

Shenzhen International Cooperation Research Project (with University of Minnesota cooperation) (grant number GJHZ20180928115030292), Shenzhen San-ming Project, Shenzhen Key Medical Discipline Construction Fund, Shenzhen High-Level Hospital Struction Fund, Research Foundation of University Shenzhen Hospital.

## Abstract

Breast cancer (BC) is a serious threat to women's health worldwide. Non-SMC condensin I complex subunit D2 (NCAPD2) is a regulatory subunit of the coagulin I complex, which is mainly involved in chromosome coagulation and separation. The clinical significance, biological behavior, and potential molecular mechanism of NCAPD2 in BC were investigated in this study. We found that NCAPD2 was frequently overexpressed in BC, and it had clinical significance in predicting the prognosis of BC patients. Moreover, loss-of-function assays demonstrated that NCAPD2 knockdown restrained the progression of BC by inhibiting proliferation and migration and enhancing apoptosis *in vitro*. It was further confirmed that the downregulation of NCAPD2 inhibited tumor growth *in vivo*. NCAPD2 promoted the progression of BC through the extracellular signal-regulated kinase 5 (ERK5) signaling pathway. Additionally, NCAPD2 could transcriptionally activate CDK1 by interacting with E2F transcription factor 1 (E2F1) in MDA-MB-231 cells. Overexpression of CDK1 alleviated the inhibitory effects of NCAPD2 knockdown in BC cells. In summary, the NCAPD2/E2F1/CDK1 axis may play a role in promoting the progression of BC, which may provide a blueprint for molecular therapy.

## KEYWORDS

BC, CDK1, migration, NCAPD2, proliferation, transcriptional regulation

Jinsong He, Rui Gao, and Jianbo Yang are the first authors with equal contributions.

This is an open access article under the terms of the [Creative Commons Attribution-NonCommercial-NoDerivs](https://creativecommons.org/licenses/by-nc-nd/4.0/) License, which permits use and distribution in any medium, provided the original work is properly cited, the use is non-commercial and no modifications or adaptations are made.

© 2022 The Authors. *Cancer Science* published by John Wiley & Sons Australia, Ltd on behalf of Japanese Cancer Association.

## 1 | INTRODUCTION

Breast cancer (BC) is a serious threat to women's health worldwide.<sup>1</sup> Triple-negative breast cancer (TNBC) is a subtype of BC with deficient expression of estrogen receptor (ER), progesterone receptor (PR), and HER2 proteins, which stands out for its high molecular heterogeneity and metastasis potential.<sup>2</sup> Breast cancer is usually treated by a combination of lumpectomy surgery, radiotherapy, and chemotherapy.<sup>3</sup> Nonetheless, these traditional treatments obviously do not meet the needs of patients.<sup>4</sup> In order to improve the prognosis and survival of patients with BC, some novel therapies, such as molecular targeted therapy, immunotherapy, nutritional therapy, and ncRNA-based therapy, have been gradually developed and explored.<sup>5-7</sup> In particular, molecular targeted therapy has become a research hotspot because of its advantages of no damage to healthy cells.<sup>8</sup> At present, some targeted therapies such as tamoxifen, sulphoraphane, and AIs are not effective in the treatment of BC.<sup>9-11</sup> Therefore, it is of great significance to find new and effective targeted therapies for BC.

Non-SMC condensin I complex subunit D2 (NCAPD2), located on chromosome 12p13.3, is a large protein complex involved in chromosome condensation.<sup>12</sup> The carboxyl terminal of NCAPD2 contains a dichotomous localization signal, which is necessary for nuclear and chromosome localization of condensin I.<sup>13</sup> In addition, NCAPD2 is involved in the assembly and separation of chromosomes during mitosis and meiosis, which is consistent with its location.<sup>14</sup> Moreover, the abnormality of NCAPD2 has been found to be significantly correlated with microcephaly, Parkinson's disease, and Alzheimer's disease.<sup>15-17</sup> Furthermore, NCAPD2 and NCAPD3 induce inflammation through the IKK/NF- $\kappa$ B pathway in ulcerative colitis.<sup>18</sup> Recently, Zhang, et al. reported that NCAPD2 is a prognostic factor in BC due to the ability to promote cell cycle and enhance invasion.<sup>19</sup> However, the potential molecular mechanism of NCAPD2 involvement in the regulation of BC remains to be elucidated.

The study aimed to explore the molecular mechanism of NCAPD2 in BC. First, the expression of NCAPD2 in BC patients was estimated by immunohistochemical (IHC) staining, and its relationship with clinicopathological features was analyzed using univariate and multivariate analyses of various potential prognostic factors and Kaplan-Meier survival analysis. In addition, the proliferation, cloning, apoptosis, cycle, and migration of BC cells were investigated by shRNA-mediated NCAPD2 knockdown. Subsequently, the molecular mechanism of NCAPD2 involvement in the regulation of BC was preliminarily evaluated.

## 2 | MATERIALS AND METHODS

### 2.1 | Tissue sample collection and IHC staining

Tumor tissue ( $n = 153$ ) and para-carcinoma tissue ( $n = 11$ ) from BC patients (Shanghai Xinchao Biotechnology) constituted tissue microarrays for immunohistochemical staining. In addition, tissue microarrays included detailed clinicopathological data such as histological classification and pathological grade. This study was approved by the Research

Ethics Committee of the Peking University Shenzhen Hospital. The tissue chips were dewaxed, repaired with citric acid antigen, and blocked by animal serum. Subsequently, they were first incubated with primary antibodies (Table S1) and then with HRP-conjugated antibody at 37°C for 2 hours. After that, the tissue chips were stained with DAB and hematoxylin (Baso, Cat. No. BA4022) in turn. Additionally, the IHC scores were determined by three pathologists according to staining percentage scores (classified as: 1 [1%-24%], 2 [25%-49%], 3 [50%-74%], 4 [75%-100%]) and staining intensity scores (scored as 0: signal less color, 1: brown, 2: light yellow, 3: dark brown). The median of IHC score determined the high or low expression of NCAPD2 in BC.

### 2.2 | Cell culture

The cell lines BT549, HS578T, MCF-7, and MDA-MB-231 were obtained from Cell Bank of the Chinese Academy of Sciences, which were cultivated in a 37°C incubator under the conditions of 5% CO<sub>2</sub> and 95% humid air. Breast cancer cell lines BT549 and MDA-MB-231 were cultured in RPMI medium supplemented with 10% FBS and 100  $\mu$ g/ml penicillin-streptomycin. HS578T and MCF-7 cells were maintained in MEM containing 10% FBS, 100  $\mu$ g/ml streptomycin, and 100 U/ml of penicillin G.

### 2.3 | RNA interference and overexpression

Three RNA interference (RNAi) sequences shNCAPD2-1, 2, 3 and shCDK1-1, 2, 3 (Table S2) were designed according to the NCAPD2/CDK1, respectively. The NCAPD2/CDK1 target sequence with the highest knockdown efficiency was ligated to the lentivirus vector BR-V-108 or LV-004 (Shanghai Yiberui Biomedical Technology) with green fluorescent protein (GFP) tags. Similarly, the amplified sequences of NCAPD2 and CDK1 were linked to the lentiviral vector. The  $1 \times 10^8$  TU/ml lentiviral vectors were transfected with BT549 or MDA-MB-231 cells ( $2 \times 10^5$  cells/ml) using Lipofectamine 3000 (Invitrogen) in RPMI with 10% FBS at 10 multiplicity of infection (MOI) for 30 minutes at 37°C. Seventy-two hours after transfection, the lentiviral vector labeled with GFP and resistance tag (Puromycin, 400 ng/ml) was used to select the cells.

It is worth noting that shCtrl is used as a negative control; shNCAPD2 is NCAPD2 knockdown; shCDK1 is CDK1 knockdown; NC(OE+KD) is an empty vector as a negative control; shCDK1+shNCAPD2 is the simultaneous knockdown of CDK1 and NCAPD2; CDK1+NC-KD is CDK1 overexpression; shNCAPD2+NC-OE is NCAPD2 knockdown; CDK1+shNCAPD2 is NCAPD2 downregulated and CDK1 overexpressed.

### 2.4 | Quantitative polymerase chain reaction (qPCR)

The cell RNA of BT549 and MDA-MB-231 was extracted with Trizol reagent (Sigma, Cat. No. T9424-100m) and reverse-transcribed

to cDNA by Hiscript QRT supermix (Vazyme, Cat. No. R123-01), respectively. The qPCR was accomplished using SYBR premix (Vazyme) and primer (Table S3). Finally, the relative mRNA expression of NCAPD2/CDK1 was accessed by  $2^{-\Delta\Delta C_t}$ .

## 2.5 | Western blotting (WB)

After the cells BT549 and MDA-MB-231 had been lysed, the protein was obtained, and the protein quality was detected using BCA protein detection kit (HyClone-Pierce). The 10- $\mu$ g protein was separated by SDS-PAGE (Invitrogen), transferred to the PVDF membrane, and then sealed with TBST solution. Subsequently, the protein was first incubated with primary antibody at 37°C for 2 hours (Table S1), and then with secondary antibody at 4°C overnight. Finally, the Millipore Immobilon Western Chemiluminescent HRP Substrate kit (Millipore, Cat. No. RPN2232) was used for color rendering and chemiluminescent imager (GE, Cat. No. AI600) observation.

## 2.6 | Proliferation assays

BT549 and MDA-MB-231 were continuously cultured to a cell density of up to 2000 cells per well. Next day, the cells were counted by Celigo (Nexcelom) at the same time every day for consecutive 5 days. In addition, the cell proliferation ability was tested after the cells were treated with BIX02189. Notably, BIX02189 (ChemeGen, Cat. No. C101208) is a potent and selective extracellular signal-regulated kinase 5 (ERK5) inhibitor with an IC50 of 1.5 nM.<sup>20</sup> Subsequently, the number of green fluorescent cells in each scanning orifice plate was accurately calculated, and the cell proliferation curve was drawn. After 14 days, the cells were first fixed with 4% paraformaldehyde for 60 minutes and then stained with Giemsa solution for 20 minutes; finally, cell clones were photographed.

## 2.7 | Flow cytometry

Cell apoptosis and cell cycle of BT549 and MDA-MB-231 were analyzed by flow cytometry, respectively. The cells were continuously cultured for 7 days in a six-well plate, centrifuged, eluted with precooled D-Hanks (pH = 7.2–7.4) for precipitation, and resuscitated with  $1 \times$  binding buffer. After the cells were stained with Annexin V-APC, the apoptosis rate was analyzed and calculated by flow cytometry. Notably, the values of the upper and lower quadrants on the right side of the figure were regarded as the apoptotic rate.

After centrifugation, the cells were washed with precooled PBS (pH = 7.2–7.4) and fixed with 70% ethanol for 2 hours. Subsequently, the cells were recentrifuged to remove the fixed solution and stained with  $40 \times$  PI mother solution. Finally, the cell was filtered in the tube of the flow machine with a pass rate of 200–350 cell/s, and

the cycle distribution was estimated. The value of the histogram is the average value in three independent experiments.

## 2.8 | Migration assays

Cell migration of BT549 and MDA-MB-231 was assessed by wound-healing assay and Transwell assay, respectively. The cells were cultured in both a 96-well plate and a well-hydrated chamber (3422 corning) with a density of  $5 \times 10^4$  cells/well, respectively.

After the low concentration of serum medium was replaced the next day, the scratches were formed by nudging upward at the center of the lower end of the 96-well plate with a scratch meter. Cellomics (Thermo) was performed to scan the 96-well plate at 4, 24, and 48 hours. Finally, the migration area was calculated and analyzed.

The inner chamber contained 100  $\mu$ l of serum-free medium and the external chamber contained 600  $\mu$ l 30% FBS. After the cell suspension had been diluted with serum-free medium, cells were added to each chamber for 24-hour cultivation. The migrating cells were fixed with 4% formaldehyde and photographed after Giemsa staining to analyze the migration fold change.

## 2.9 | Mouse xenograft model

All procedures involving mice and experimental protocols were approved by the Institutional Animal Care and Use Committees of Peking University Shenzhen Hospital. Four-week-old female BALB/ C nude mice were purchased from Beijing Viton Lihua Laboratory Animal Technology Co., LTD, which were randomly divided into shCtrl ( $n = 10$ ) and shNCAPD2 ( $n = 10$ ) groups. Data were collected 25 days after MDA-MB-231 cells (with or without NCAPD2 knockdown) had been injected subcutaneously into the mice. In vivo imaging was performed once a week to detect tumor formation and record fluorescence intensity. At the same time, the tumor volume of mice was collected once or twice every other week, ensuring at least five measurements. After 72 days, the mice were sacrificed, and the tumors were taken and weighed for preservation. Tumor tissues were extracted from mice and stained with Ki67 (antibody information is shown in Table S1) to further analyze the effects of NCAPD2 knockdown on BC.

## 2.10 | Affymetrix human gene chip prime view

In this project, Affymetrix human Gene Chip Prime View combined with Affymetrix Scanner 3000 was performed to analyze the molecular mechanism, and the outcomes were guided by the manufacturer. Accordingly, the volcano plot and hierarchical clustering of the shCtrl and shNCAPD2 in MDA-MB-231 cells were presented by the differentially expressed genes (DEGs) with criterion of  $|\text{Fold Change}| \geq 1.3$  and false discovery rate (FDR)  $< 0.05$ . Furthermore, the significant enrichment of DEGs in classical pathways, disease, and function were demonstrated based on ingenuity pathway analysis (IPA).

## 2.11 | Bioinformatics analysis

To clarify the impact of NCAPD2 knockdown on downstream signaling pathways, the Database for Annotation Visualization and Integrated Discovery (DAVID, <https://david.ncifcrf.gov/>) was applied to analyze the Kyoto Encyclopedia of Genes and Genomes (KEGG).

## 2.12 | Dual-luciferase assay

Promoter deletion was analyzed using a dual-luciferase reporting system following the methods provided in the literature.<sup>21</sup> The CDK1 promoter region fragment (chr10:60776478-60794852) was amplified and cloned into the luciferase reporter vector GL002 (Promega), designated as GL002-CDK1. Mutant construct GL002-CDK1-MUT was generated by site-directed mutagenesis and GL002-CDK1-WT as negative control. According to the instructions of Promega dual-luciferase system (Cat. No. E2940), Firefly luciferase value and Renilla luciferase signals were determined. Each experimental analysis was repeated three times.

## 2.13 | Chromatin immunoprecipitation (ChIP)-qPCR assay

ChIP-qPCR assay was performed as described previously.<sup>22</sup> MDA-MB-231 cells with NCAPD2 overexpression were cross-linked with formaldehyde, lysed in SDS buffer, and sheared mechanically by sonication to fragment the DNA. Protein-DNA complexes were precipitated with 2 µg control normal mouse IgG (Sigma, Cat. No. I5381), 2 µg Histone H3 (D2B12) XP<sup>®</sup> Rabbit mAb (CST, Cat. No.4620), and 4 µg anti-E2F1 (Proteintech, Cat. No. 66515-1-Ig) antibody, respectively. After separating the complex from the antibody, the primers specific for CDK1 promoter and SYBR premix (Vazyme) were used to detect the eluted DNA fragment. The primer sequence for CDK1 was as follows: 5'-AAGAAGAACGGAGCGAACAGTAG-3' and 5'-AGGAAAGGGCGCTAGAGAAA-3'.

## 2.14 | Statistical analysis

All data were presented as mean ± standard deviation and analyzed using GraphPad Prism Version 8.0. The statistical significance between different groups was evaluated using the unpaired Student *t* test, and *p* < 0.05 was considered statistically significant.

Univariate and multivariate analyses of various potential prognostic factors in BC patients were performed using the Cox regression model. The prognostic value was calculated by Kaplan-Meier analysis with log-rank test. The relative mRNA expression was accessed by  $2^{-\Delta\Delta Ct}$ .

## 3 | RESULTS

### 3.1 | Clinical correlation between NCAPD2 and BC

In this study, the association of NCAPD2 with clinicopathological features of BC was analyzed. Among the 174 cases examined, high expression of NCAPD2 was observed in 66 cases (43.1%), but not in matched normal tissues (Table 1). Moreover, the typical representative pictures of IHC staining showed that the number of stained positive cells in tumor tissues was significantly higher than that in paired normal tissues, indicating that NCAPD2 was abundantly expressed in BC (Figure 1A). In this study, tumor node metastasis (TNM) classification, which is a staging system in oncology (T is primary tumor, N is lymph node, and M is distant metastasis), was performed according to the seventh edition of the Union for International Cancer Control (UICC).<sup>23</sup> Mann-Whitney U analysis showed expression of NCAPD2 was associated with lymphatic metastasis (Table 2). Moreover, univariate and multivariate analyses were performed on various potential prognostic factors of BC patients through the Cox regression model. There was a significant correlation between the expression level of NCAPD2 and TNM of BC patients, which indicated that the patients with higher NCAPD2 expression had a poorer survival prognosis (Table 3). In addition, according to the Kaplan-Meier survival analysis, there was a significant negative correlation between the expression of NCAPD2 and the overall survival of BC (Figure 1B). The increased expression of NCAPD2 indicated the shortening of the survival time of BC patients. Collectively, NCAPD2 was frequently overexpressed in BC, and it had clinical significance in predicting the prognosis of BC patients.

### 3.2 | Knockdown of NCAPD2 inhibits the malignant phenotypes of BC in vitro

The expression of NCAPD2 was moderate in BT549 and highly enriched in MDA-MB-231 cells (Figure S1A). Subsequently, the targeted sequence shNCAPD2-3 was used to infect BT549 and MDA-MB-231 to downregulate the expression of NCAPD2

TABLE 1 Expression patterns in breast cancer tissues and paracarcinoma tissues revealed in immunohistochemistry analysis

NCAPD2 expression	Tumor tissue		Paracarcinoma tissue		P value
	Cases	Percentage	Cases	Percentage	
Low	87	56.9%	11	100%	<0.001
High	66	43.1%	0	-%	

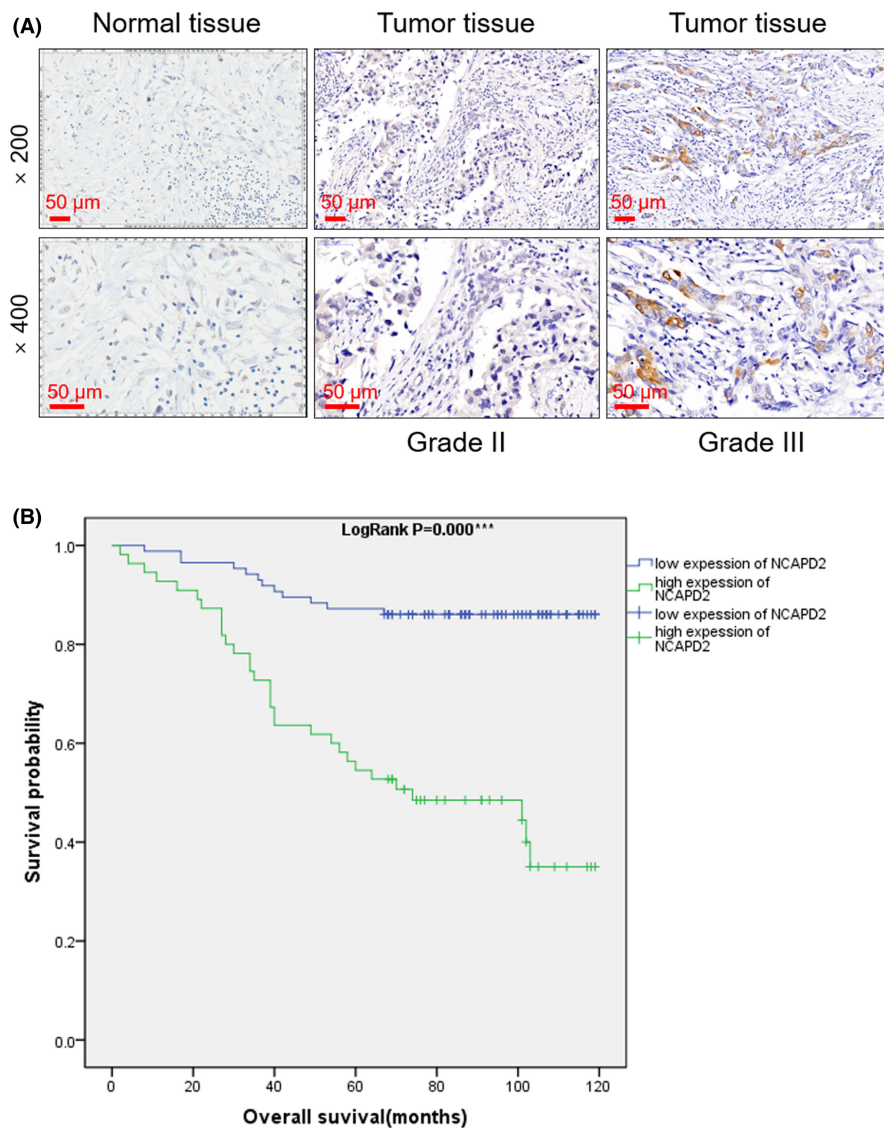


**FIGURE 1** The relationship between the expression of non-SMC condensin I complex subunit D2 (NCAPD2) and breast cancer (BC). A, Representative pictures of the expression levels of NCAPD2 in normal tissues and tumor tissues with different grades detected by immunohistochemistry (IHC) (200× and 400× magnification). B, Relationship between the expression of NCAPD2 and the overall survival of BC patients

(Figure S1B). The infection efficiency and knockdown efficiency were measured in turn to determine the successful knockdown of NCAPD2 in BT549 and MDA-MB-231 (Figure S1C–E). Next, the differences in proliferation, apoptosis, and migration between groups of shCtrl and shNCAPD2 were estimated by BT549 and MDA-MB-231 cells. The results of cells counting for 5 days showed that the cell number in the shNCAPD2 group was remarkably lower than that in the shCtrl group, reflecting the inhibition of cell proliferation by NCAPD2 knockdown (Figure 2A). In addition, the downregulation of NCAPD2 led to a sharp increase in the apoptosis rate of BT549 and MDA-MB-231 (Figure 2B). As illustrated in Figure 2C, cells in the shNCAPD2 group were repressed in the G2 phase compared with the control group, which indirectly indicated the weakening of proliferation ability. As expected, both the migration rate (Figure 2D) and the migration multiples (Figure 2E) in the shNCAPD2 group were significantly lower than those in the control group. Comprehensive analysis demonstrated that NCAPD2 knockdown restrains the

progression of BC by inhibiting proliferation and migration and enhancing apoptosis in vitro.

### 3.3 | Knockdown of NCAPD2 suppresses tumor growth in vivo

The effects of downregulation of NCAPD2 were further analyzed by the construction of a mouse xenograft model. The typical images of mice clearly showed that the fluorescence intensity of the shNCAPD2 group was weaker than that of the control group (Figure 3A). Additionally, observations lasting for 70 days indicated that the volume of the shNCAPD2 group was always smaller than that of the shCtrl group (Figure 3B). Moreover, there was a significant difference in the size (Figure 3C) and weight (Figure 3D) of the removed tumor between the shNCAPD2 group and the shCtrl group. In addition, fewer positive cells with Ki67 staining were detected in

**TABLE 2** Relationship between NCAPD2 expression and tumor characteristics in patients with breast cancer

Features	No. of patients	NCAPD2 expression		P value
		low	high	
All patients	141	86	55	
Age (years)				0.811
<58	70	42	28	
≥58	71	44	27	
Grade				0.443
I	1	0	1	
II	69	42	27	
III	61	40	21	
T cells infiltrate				0.422
T1	36	22	14	
T2	86	56	30	
T3	13	5	8	
T4	2	1	1	
Lymphatic metastasis (N)				0.041
N0	74	50	24	
N1	34	23	11	
N2	19	8	11	
N3	12	5	7	
Stage				0.081
1	24	13	11	
2	75	56	19	
3	37	15	22	

shNCAPD2 tumor tissues (Figure 3E,F). Not surprisingly, knockdown of NCAPD2 inhibited tumor generation in vivo.

### 3.4 | NCAPD2 promotes the progression of BC through the ERK5 signaling pathway

We performed Affymetrix Human Gene Chip Prime View analysis on MDA-MB-231 cells to further clarify the mechanism of NCAPD2 regulating BC. The multiples and significance of DEGs between the shCtrl and shNCAPD2 groups were tested, and significant differences were shown by volcano maps (Figure S2A). We found that these DEGs were significantly enriched in the ERK5 signaling pathway through IPA (Figure S2B). In addition, KEGG term pathway enrichment analysis was conducted between the shCtrl and shNCAPD2 groups, revealing the top 10 enrichment-related pathways, and the ERK5 signaling pathway was the first-ranked signaling pathway (Figure 4A). Additionally, BT549 and MDA-MB-231 cells overexpressing NCAPD2 were treated with ERK5 inhibitors (BIX02189, 10 μM) to clarify the role of the ERK5 signaling pathway in BC. The NCAPD2 group contained cells with NCAPD2 overexpression, and

**TABLE 3** Relationship between NCAPD2 expression and tumor characteristics in patients with breast cancer

		NCAPD2
Lymphatic metastasis(N)	Pearson correlation	0.174
	Significance (double-tail)	0.041
	N	139

the control group was the negative control. Compared with the control group, cell proliferation slowed down after treatment with BIX02189. The addition of BIX02189 alleviated the promotion effect of NCAPD2 overexpression on BC cell proliferation (Figure 4B). The apoptosis rate of MDA-MB-231 cells was enhanced by treatment with ERK5 inhibitor BIX02189. Compared with the control group, NCAPD2 overexpression attenuated the apoptotic sensitivity of BC cells. BIX02189 could reverse the sensitivity of NCAPD2 overexpression to BC cell apoptosis (Figure 4C). Therefore, NCAPD2 may play a role in promoting BC progression via the ERK5 signaling pathway.

### 3.5 | NCAPD2 regulates the expression of CDK1 through E2F1 transcription

According to the results of hierarchical clustering, 579 genes were up-regulated and 885 genes were downregulated after NCAPD2 knockdown in MDA-MB-231 cells (Figure 5A). In addition, these DEGs were enriched in diseases and functions such as cancer, cell death and survival, and cell cycle (Figure S2C). Furthermore, the DEGs with the most significant differential multiples were further screened by qPCR (Figure S2D) and WB (Figure S2E). These results indicated that the expression of CDK1 was decreased at both mRNA and protein levels. Moreover, we identified that the function of DEG enrichment was related to cancer and cell cycle. As it is known, CDK1 plays a key role in cell cycle progression.<sup>24</sup> More importantly, CDK1 is a typical cancer-promoting factor in BC.<sup>25</sup> In view of the facts, we preliminarily assumed that CDK1 was the downstream target of NCAPD2.

In order to verify our hypothesis, we carried out the following experiments. Through the analysis of the database ([https://www.grnpedia.org/trust/result\\_tonly.php?gene=CDK1&species=human&confirm=](https://www.grnpedia.org/trust/result_tonly.php?gene=CDK1&species=human&confirm=)), we found that E2F1 was one of the transcriptional activators of CDK1.<sup>26</sup> Subsequently, we scanned the CDK1 promoter region with the canonical binding DNA motifs of E2F1 (5'-GTTGGCGC-3') and found such a motif between -1825 and -1832 upstream of the transcription start site, indicating that E2F1 regulated CDK1 promoter activity (Figure 5B). Additionally, the Co-IP assay showed that there was an interaction between NCAPD2 and E2F1, suggesting that NCAPD2 could directly bind to the E2F1 protein in MDA-MB-231 cells (Figure 5C). Accordingly, we inferred that NCAPD2 may regulate the expression of CDK1 through E2F1. Furthermore, dual-luciferase assay was performed to explore whether NCAPD2 regulated E2F1-mediated change of CDK1 promoter activity. We generated a luciferase reporter construct with

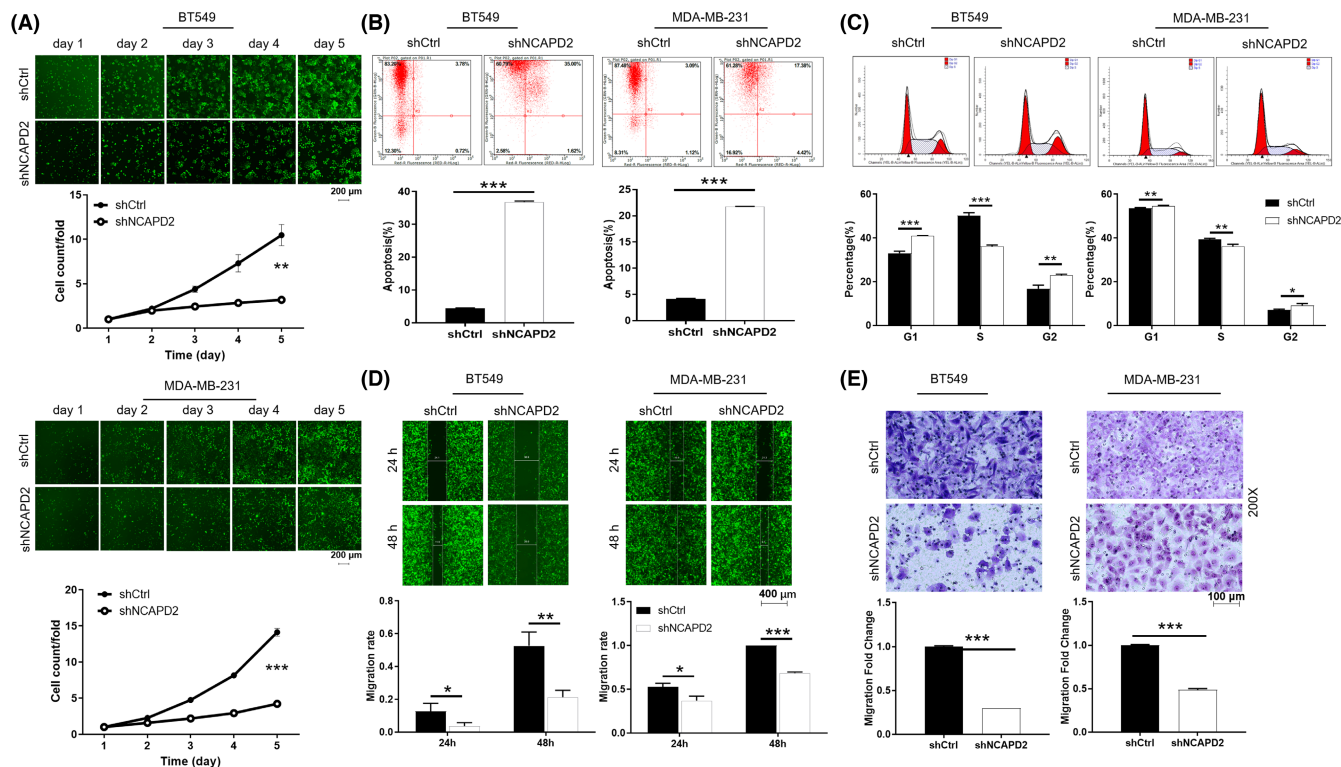


**FIGURE 2** Non-SMC condensin I complex subunit D2 (NCAPD2) knockdown inhibits progression of breast cancer (BC) in vitro. A, The Celigo assay was employed to show the effects of NCAPD2 on cell proliferation of BT549 and MDA-MB-231 cells. B, C, Flow cytometry was performed to analyze cell apoptosis (B) and cycle distribution (C) of BT549 and MDA-MB-231 cells with or without NCAPD2 knockdown. D, E, BT549 and MDA-MB-231 cell migration ability was accessed by wound-healing assay (D) and Transwell assay (E). Representative images were selected from at least three independent experiments. Data are shown as mean  $\pm$  SD. \* $p < 0.05$ , \*\* $p < 0.01$ , \*\*\* $p < 0.001$

wild-type (WT) and E2F1 binding motif-mutated CDK1 promoter (MUT). NCAPD2 expression significantly increased CDK1 promoter-driven luciferase activity in the WT group but not the MUT group. The results suggested that NCAPD2 overexpression promoted the binding of E2F1 to the CDK1 promoter in MDA-MB-231 cells (Figure 5D). In addition, we performed ChIP-qPCR assay and confirmed that E2F1 promoted CDK1 transcription, and overexpression of NCAPD2 accelerated this transcription (Figure 5E). Collectively, our findings supported the view that NCAPD2 could transcriptionally activate CDK1 by interacting with E2F1 in MDA-MB-231 cells.

### 3.6 | Overexpression of CDK1 alleviates the inhibitory effects of NCAPD2 knockdown in BC cells

Loss/gain function assays were conducted to determine whether CDK1 was involved in the cellular behaviors. As illustrated in Figure S3A-F, MDA-MB-231 cells with deletion of CDK1 (shCDK1) and CDK1 + NCAPD2 (shCDK1+shNCAPD2) were established, respectively. As expected, CDK1 knockdown indeed inhibited proliferation and migration and enhanced the susceptibility to apoptosis in MDA-MB-231 cells. Simultaneous downregulation of CDK1 and NCAPD2 could strengthen the inhibitory effects on malignant behaviors (Fig S4A-E). Moreover, CDK1 overexpression

and NCAPD2 knockdown were established in MDA-MB-231 cell lines (Figure S5A-B). NC(OE+KD) is an empty vector as a negative control; CDK1+NC-KD is CDK1 overexpression; shNCAPD2+NC-OE is NCAPD2 knockdown; CDK1+shNCAPD2 is NCAPD2 down-regulated and CDK1 overexpressed. Obviously, overexpression of CDK1 promoted malignant progression of MDA-MB-231 cells, such as increasing proliferation, decreasing apoptosis, and improving migration. Further analysis showed that NCAPD2 knockdown partially reversed the promotion effect of CDK1 on BC cells (revised Figure 5F-I). Furthermore, loss/gain function assays demonstrated that CDK1 knockdown partially attenuated the effect of NCAPD2 overexpression on the growth and migration inhibition of MDA-MB-231 cells (Figure S6A-B). Collectively, NCAPD2 played a role in promoting malignant progression of BC through CDK1.

## 4 | DISCUSSION

On the one hand, BC is not only invasive and highly heterogeneous but also lacks effective therapy.<sup>4</sup> On the other hand, NCAPD2 is involved in the assembly and separation of chromosomes during cell mitosis,<sup>14</sup> which may be associated with the biological processes of cancer cells.<sup>18,27</sup> Recently, NCAPD2 has been reported as a prognostic factor for promoting cell cycle and invasion in BC.<sup>19</sup> Nonetheless,

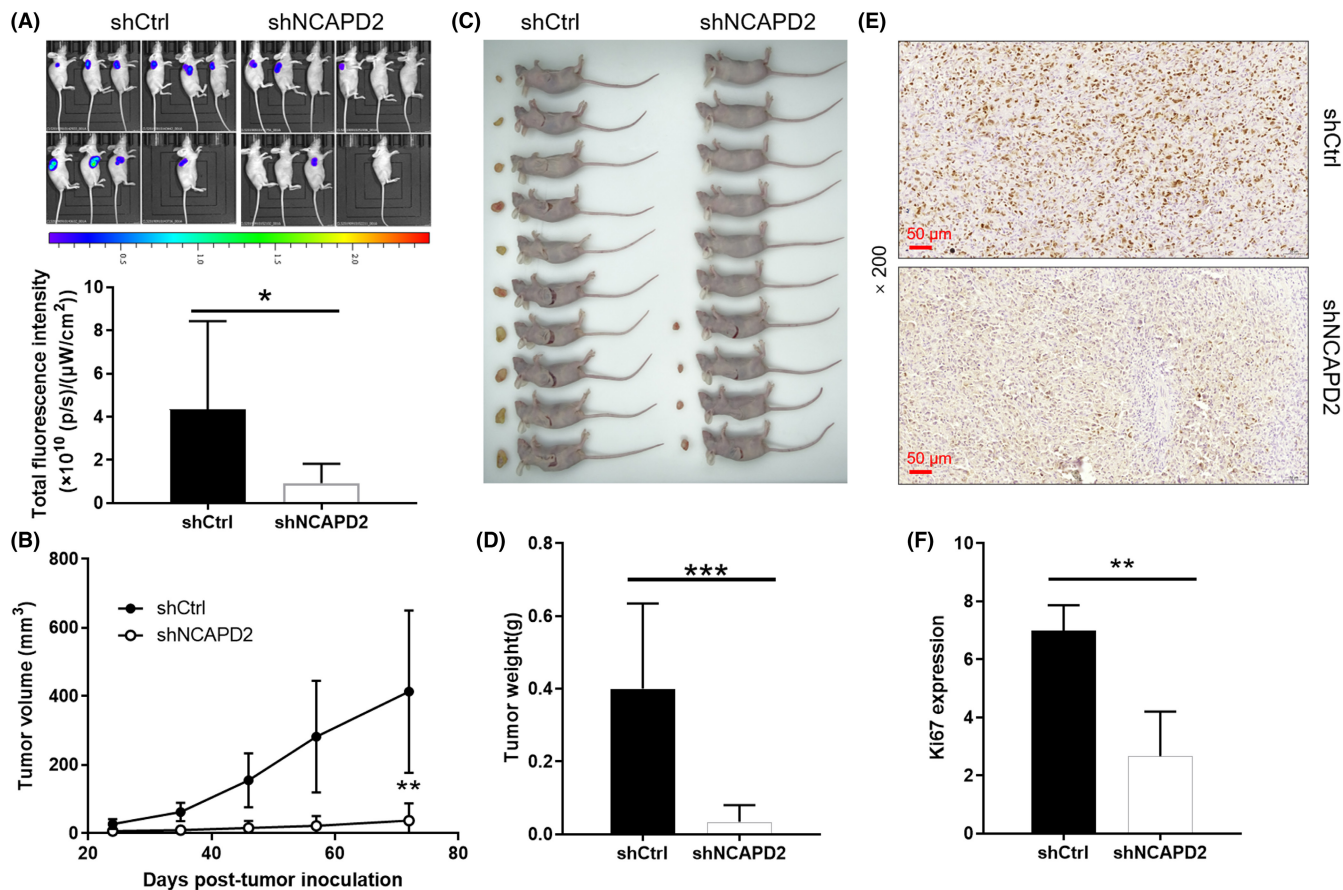


**FIGURE 3** Non-SMC condensin I complex subunit D2 (NCAPD2) knockdown inhibits tumor formation of breast cancer (BC) in vivo. A, In vivo imaging was performed to evaluate the tumor burden in mice of the shNCAPD2 and shCtrl groups post tumor inoculation (fluorescence intensity was scanned and used as a representation of tumor burden). B, MDA-MB-231 cells with or without NCAPD2 knockdown; the volume was measured and calculated at indicated time intervals. C, Photos of the removed tumors were taken post tumor inoculation. D, Average weight of tumors between the shNCAPD2 and shCtrl groups. E, The Ki67 level in tumors removed from mice was detected by immunohistochemistry (IHC) as a representation of tumor growth. F, Ki67 expression difference between the shNCAPD2 and shCtrl groups. Data are shown as mean  $\pm$  SD. \* $p < 0.05$ , \*\* $p < 0.01$ , \*\*\* $p < 0.001$ .

the underlying molecular mechanism of NCAPD2 involvement in the regulation of BC remains to be elucidated. In this context, we found that NCAPD2 was highly expressed in BC. High expression of NCAPD2 predicted poor clinical prognosis in BC patients. Moreover, knockdown of NCAPD2 restrained the progression of BC by inhibiting proliferation and migration and enhancing apoptosis in vitro. It was further confirmed that the downregulation of NCAPD2 inhibited tumor generation in vivo. Collectively, we elucidated the promoting role of NCAPD2 in BC.

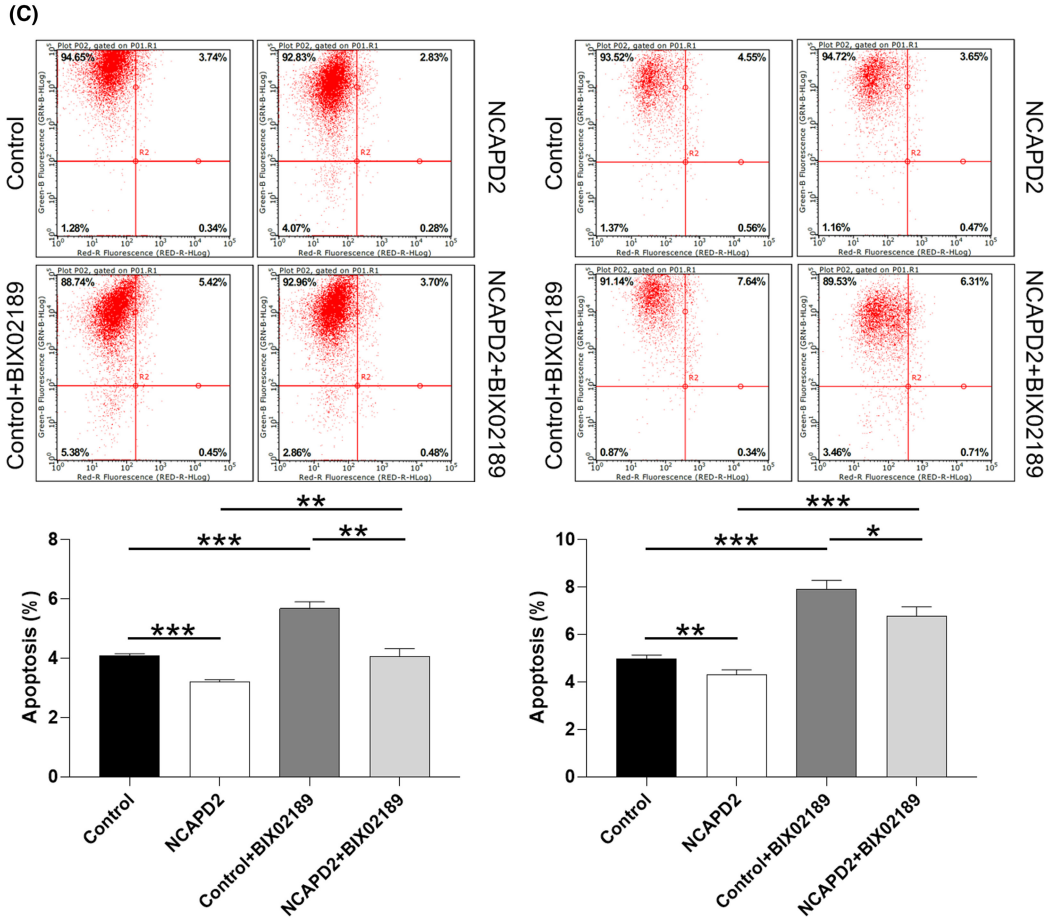
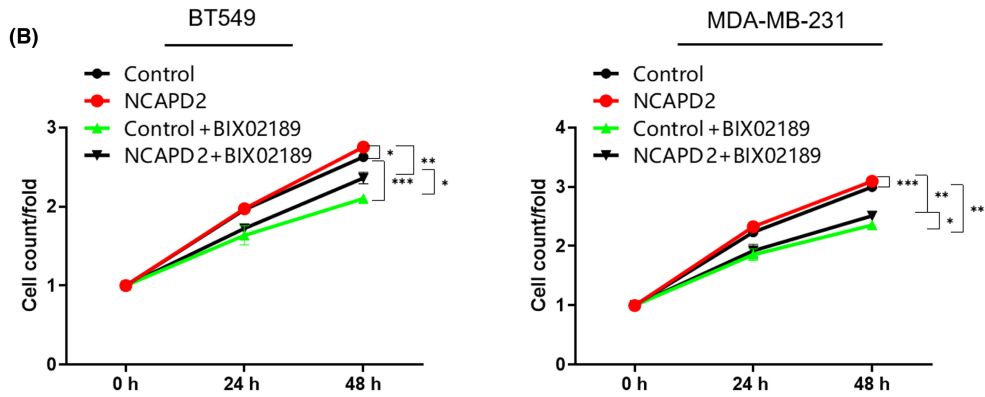
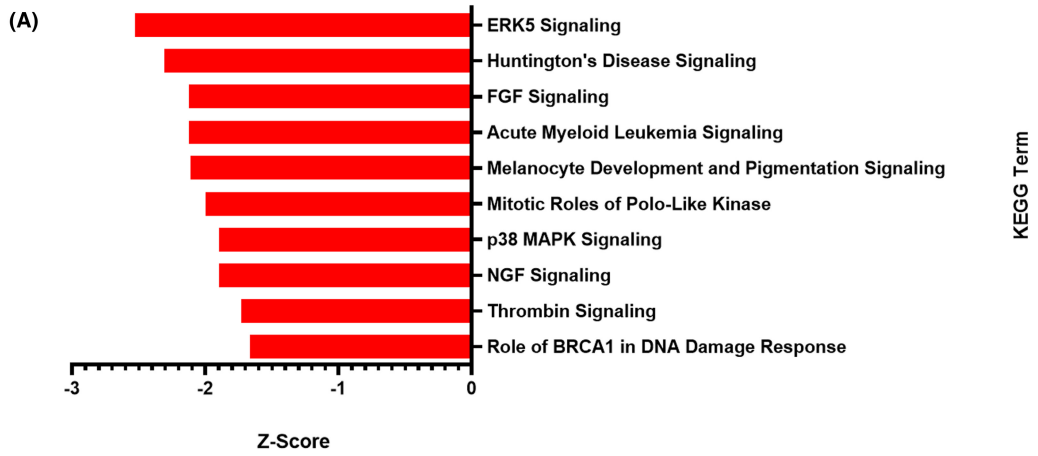
Additionally, the regulatory mechanism of NCAPD2 in BC progression was preliminarily explored. NCAPD2 knockdown resulted in significant enrichment of the ERK5 signaling pathway. Previous

study reported that the ERK5 signaling pathway played an important role in inducing and maintaining migration and invasion of BC cells.<sup>28</sup> Inhibition of the MEK5/ERK5 signaling pathway could reduce the proliferation and survival of BC.<sup>29</sup> Consistently, the present study demonstrated that inhibition of the ERK5 inhibitor could inhibit BC cell proliferation and enhance apoptosis. Moreover, inhibition of the ERK5 signaling pathway alleviated the promotion effect of NCAPD2 overexpression on BC progression. We revealed that NCAPD2 exhibited a role in promoting BC through the ERK5 signaling pathway.

Furthermore, Affymetrix Human Gene Chip Prime View analysis and IPA identified that CDK1 is a key mediator for NCAPD2 in promoting tumor growth and migration in BC. Cyclin-dependent

**FIGURE 4** Non-SMC condensin I complex subunit D2 (NCAPD2) promotes the progression of breast cancer (BC) through the ERK5 signaling pathway. A, The potential mechanism of NCAPD2 in BC cells was analyzed by Kyoto Encyclopedia of Genes and Genomes (KEGG) enrichment analysis. The names of the enrichment pathways are shown on the left axis. The abscissa is the enrichment factor. High enrichment factor indicates that the enrichment of different proteins in this pathway is significant. B, C, The effects of NCAPD2 overexpression and ERK5 inhibitor treatment on BT549 and MDA-MB-231 cells' proliferation (B) and apoptosis (C) were detected. Representative images were selected from at least three independent experiments. Data are shown as mean  $\pm$  SD. \* $p < 0.05$ , \*\* $p < 0.01$ , \*\*\* $p < 0.001$





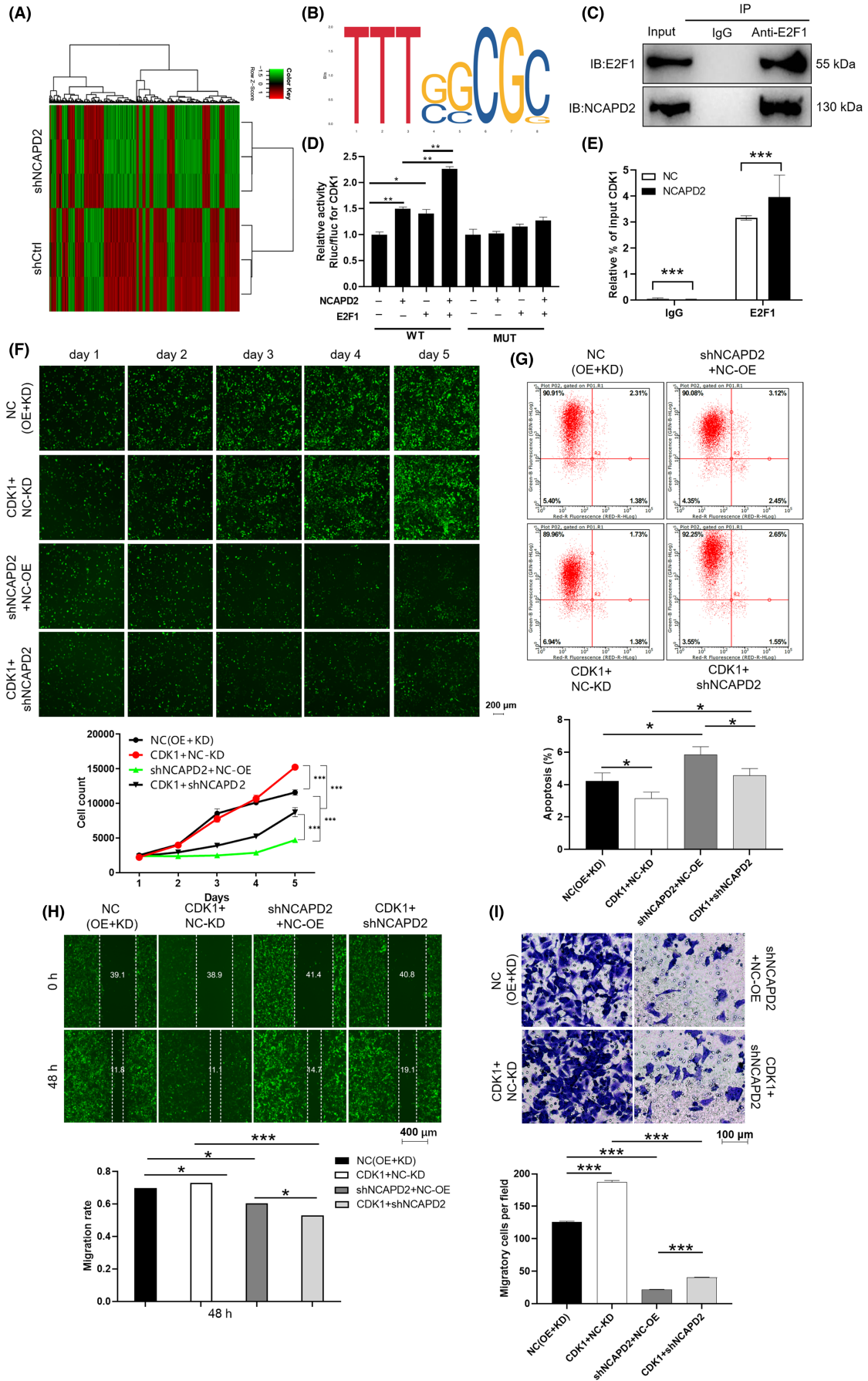


**FIGURE 5** Non-SMC condensin I complex subunit D2 (NCAPD2) regulates the expression of CDK1 through E2F1 transcription. A, Prime View Human Gene Expression Array was performed to identify the differentially expressed genes (DEGs) between the shNCAPD2 and shCtrl groups of MDA-MB-231 cells and shown by hierarchical clustering. B, Schematic of the CDK1 promoter reporter and its putative E2F1-binding site. C, The interaction between NCAPD2 and E2F1 was confirmed by Co-IP assay. D, Dual-luciferase assay was performed to explore whether NCAPD2 regulated CDK1 promoter activity. E, ChIP-qPCR assay was conducted to confirm that E2F1 bound to the CDK1 promoter. F-I, Cell models were subjected to the detection of cell proliferation (F) and cell apoptosis (G). Cell migration ability was assessed by wound-healing assay (H) and Transwell assay (I). NC(OE+KD) is an empty vector as a negative control; CDK1+NC-KD is CDK1 overexpression; shNCAPD2+NC-OE is NCAPD2 knockdown; CDK1+shNCAPD2 is NCAPD2 downregulated and CDK1 overexpressed. Representative images were selected from at least three independent experiments. Data are shown as mean  $\pm$ SD. \* $p < 0.05$ , \*\* $p < 0.01$ , \*\*\* $p < 0.001$

kinases (CDKs) are serine/threonine kinases that coregulate the cell cycle with certain regulatory cyclins.<sup>30</sup> CDK1 is the only essential CDK facilitating the G2/M and G1/S transitions as well as G1 progression.<sup>30</sup> The activity of CDK1 is strictly regulated by cyclins and checkpoint kinases such as WEE1 and Chk1 to ensure that cells do not enter mitosis if DNA replication is incomplete or damaged.<sup>31</sup> In addition, CDK1 phosphorylates a large number of proteins, promoting nuclear membrane rupture, chromatin concentration, and spindle assembly.<sup>32</sup> Considerable evidence suggested that CDK1 is not only overexpressed in some tumors (such as BC,<sup>33</sup> colorectal cancer,<sup>34</sup> lung cancer,<sup>35</sup> melanoma,<sup>36</sup> and hepatocellular carcinoma<sup>37</sup>) but is also associated with poor prognosis. Additionally, targeted CDK1 can specifically enhance the sensitivity of tumor cells to DNA damage agents without affecting the sensitivity of normal epithelial cells.<sup>38,39</sup> Inhibition of CDK1 expression is considered to be an attractive antitumor strategy.<sup>25,40,41</sup> The present study clarified the inhibitory effect of CDK1 in BC.

Previous study reported that E2F transcription factor 1 (E2F1) transcription activated CDK1.<sup>11</sup> Consistently, our data demonstrated that NCAPD2 could transcriptionally activate CDK1 by interacting with E2F1 in MDA-MB-231 cells. Furthermore, the transactivation ability of E2F1, a transcription factor involved in cell cycle regulation and apoptosis, is regulated by Rb.<sup>42</sup> Therefore, whether there is a possible interaction between NCAPD2 and Rb is an unclarified point in this study that requires to be further explored. In addition, we have identified that a variety of transcription factors may initiate and regulate the expression of CDK1 through bioinformatics analysis. Nonetheless, our data suggested that E2F1 was involved in transcriptional regulation between NCAPD2 and CDK1 as a link between NCAPD2 and CDK1. Of course, there must be a variety of other transcription factors in the promoter site of CDK1 to regulate the transduction of other signal pathways, which require in-depth exploration. Taken together, our findings revealed that NCAPD2-mediated E2F1 transcription activated CDK1 expression to promote BC progression.

NCAPD2 was frequently overexpressed in BC, and it had clinical significance in predicting the prognosis of BC patients. NCAPD2 could transcriptionally activate CDK1 by interacting with E2F1 in MDA-MB-231 cells. Knockdown of NCAPD2 inhibited the proliferation and migration of BC, and overexpression of CDK1 could alleviate these inhibitory effects. In summary, the NCAPD2/E2F1/CDK1 axis may play a role in promoting the development and progression of BC, which may provide a blueprint for molecular therapy.

## DISCLOSURE

The authors declare no conflict of interest.

## ORCID

Jinsong He  <https://orcid.org/0000-0002-0850-5260>

## REFERENCE

- Blows FM, Driver KE, Schmidt MK, et al. Subtyping of breast cancer by immunohistochemistry to investigate a relationship between subtype and short and long term survival: a collaborative analysis of data for 10,159 cases from 12 studies. *PLoS Med*. 2010;7(5):e1000279.
- Kumar P, Aggarwal R. An overview of triple-negative breast cancer. *Arch Gynecol Obstet*. 2016;293(2):247-269.
- Chang-Qing Y, Jie L, Shi-Qi Z, et al. Recent treatment progress of triple negative breast cancer. *Prog Biophys Mol Biol*. 2020;151:40-53.
- Lebert JM, Lester R, Powell E, Seal M, McCarthy J. Advances in the systemic treatment of triple-negative breast cancer. *Curr Oncol*. 2018;25(Suppl 1):S142-S150.
- Bhullar KS, Lagarón NO, McGowan EM, et al. Kinase-targeted cancer therapies: progress, challenges and future directions. *Mol Cancer*. 2018;17(1):48.
- Cyprian FS, Akhtar S, Gatalica Z, Vranic S. Targeted immunotherapy with a checkpoint inhibitor in combination with chemotherapy: A new clinical paradigm in the treatment of triple-negative breast cancer. *Bosn J Basic Med Sci*. 2019;19(3):227-233.
- Kahraman M, Röske A, Laufer T, et al. MicroRNA in diagnosis and therapy monitoring of early-stage triple-negative breast cancer. *Sci Rep*. 2018;8(1):11584.
- Lin SX, Chen J, Mazumdar M, et al. Molecular therapy of breast cancer: progress and future directions. *Nat Rev Endocrinol*. 2010;6(9):485-493.
- Xu X, Chlebowski RT, Shi J, Barac A, Haque R. Aromatase inhibitor and tamoxifen use and the risk of venous thromboembolism in breast cancer survivors. *Breast Cancer Res Treat*. 2019;174(3):785-794.
- Mangla B, Neupane YR, Singh A, Kohli K. Tamoxifen and Sulphoraphane for the breast cancer management: A synergistic nanomedicine approach. *Med Hypotheses*. 2019;132: 109379.
- Nagini S. Breast Cancer: Current Molecular Therapeutic Targets and New Players. *Anticancer Agents Med Chem*. 2017;17(2):152-163.
- Verlinden L, Eelen G, Beullens I, et al. Characterization of the condensin component Cnap1 and protein kinase Melk as novel E2F target genes down-regulated by 1,25-dihydroxyvitamin D3. *J Biol Chem*. 2005;280(45):37319-37330.
- Ball AR Jr, Schmiesing JA, Zhou C, et al. Identification of a chromosome-targeting domain in the human condensin subunit CNAP1/hCAP-D2/Eg7. *Mol Cell Biol*. 2002;22(16):5769-5781.
- Schmiesing JA, Gregson HC, Zhou S, Yokomori K. A human condensin complex containing hCAP-C-hCAP-E and CNAP1, a homolog of *Xenopus* XCAP-D2, colocalizes with phosphorylated histone H3

- during the early stage of mitotic chromosome condensation. *Mol Cell Biol.* 2000;20(18):6996-7006.
15. Bouguen G, Chevaux JB, Peyrin-Biroulet L. Recent advances in cytokines: therapeutic implications for inflammatory bowel diseases. *World J Gastroenterol.* 2011;17(5):547-556.
  16. Martin CA, Murray JE, Carroll P, et al. Mutations in genes encoding condensin complex proteins cause microcephaly through decatenation failure at mitosis. *Genes Dev.* 2016;30(19):2158-2172.
  17. Zhang P, Liu L, Huang J, et al. Non-SMC condensin I complex, subunit D2 gene polymorphisms are associated with Parkinson's disease: a Han Chinese study. *Genome.* 2014;57(5):253-257.
  18. Yuan CW, Sun XL, Qiao LC, et al. Non-SMC condensin I complex subunit D2 and non-SMC condensin II complex subunit D3 induces inflammation via the IKK/NF-kappaB pathway in ulcerative colitis. *World J Gastroenterol.* 2019;25(47):6813-6822.
  19. Zhang Y, Liu F, Zhang C, et al. Non-SMC Condensin I Complex Subunit D2 Is a Prognostic Factor in Triple-Negative Breast Cancer for the Ability to Promote Cell Cycle and Enhance Invasion. *Am J Pathol.* 2020;190(1):37-47.
  20. Tataka RJ, O'Neill MM, Kennedy CA, et al. Identification of pharmacological inhibitors of the MEK5/ERK5 pathway. *Biochem Biophys Res Commun.* 2008;377(1):120-125.
  21. Xu YZ, Kanagaratham C, Jancik S, Radzioch D. Promoter deletion analysis using a dual-luciferase reporter system. *Methods Mol Biol.* 2013;977:79-93.
  22. Asp P. How to Combine ChIP with qPCR. *Methods Mol Biol.* 2018;1689:29-42.
  23. Edge SB, Compton CC. The American Joint Committee on Cancer: the 7th edition of the AJCC cancer staging manual and the future of TNM. *Ann Surg Oncol.* 2010. ;17(6):1471-1474.
  24. Vassilev LT. Cell cycle synchronization at the G2/M phase border by reversible inhibition of CDK1. *Cell Cycle.* 2006;5(22):2555-2556.
  25. Izadi S, Nikkhoo A, Hojjat-Farsangi M, et al. CDK1 in Breast Cancer: Implications for Theranostic Potential. *Anticancer Agents Med Chem.* 2020;20(7):758-767.
  26. Yasui K, Okamoto H, Arii S, Inazawa J. Association of over-expressed TFDP1 with progression of hepatocellular carcinomas. *J Hum Genet.* 2003;48(12):609-613.
  27. Jing Z, He X, Jia Z, Sa Y, Yang B, Liu P. NCAPD2 inhibits autophagy by regulating Ca(2+)/CAMKK2/AMPK/mTORC1 pathway and PARP-1/SIRT1 axis to promote colorectal cancer. *Cancer Lett.* 2021;520:26-37.
  28. Pavan S, Meyer-Schaller N, Diepenbruck M, Kalathur RKR, Saxena M, Christofori G. A kinome-wide high-content siRNA screen identifies MEK5-ERK5 signaling as critical for breast cancer cell EMT and metastasis. *Oncogene.* 2018;37(31):4197-4213.
  29. Wright TD, Raybuck C, Bhatt A, et al. Pharmacological inhibition of the MEK5/ERK5 and PI3K/Akt signaling pathways synergistically reduces viability in triple-negative breast cancer. *J Cell Biochem.* 2020;121(2):1156-1168.
  30. Malumbres M. Cyclin-dependent kinases. *Genome Biol.* 2014;15(6):122.
  31. Nigg EA. Mitotic kinases as regulators of cell division and its checkpoints. *Nat Rev Mol Cell Biol.* 2001;2(1):21-32.
  32. London N, Biggins S. Signalling dynamics in the spindle checkpoint response. *Nat Rev Mol Cell Biol.* 2014;15(11):736-747.
  33. Sung WW, Lin YM, Wu PR, et al. High nuclear/cytoplasmic ratio of Cdk1 expression predicts poor prognosis in colorectal cancer patients. *BMC Cancer.* 2014;14:951.
  34. Li M, He F, Zhang Z, Xiang Z, Hu D. CDK1 serves as a potential prognostic biomarker and target for lung cancer. *J Int Med Res.* 2020;48(2):300060519897508.
  35. Kuang Y, Guo W, Ling J, et al. Iron-dependent CDK1 activity promotes lung carcinogenesis via activation of the GP130/STAT3 signaling pathway. *Cell Death Dis.* 2019;10(4):297.
  36. Ravindran Menon D, Luo Y, Arcaroli JJ, et al. CDK1 Interacts with Sox2 and Promotes Tumor Initiation in Human Melanoma. *Cancer Res.* 2018;78(23):6561-6574.
  37. Yang WX, Pan YY, You CG. CDK1, CCNB1, CDC20, BUB1, MAD2L1, MCM3, BUB1B, MCM2, and RFC4 May Be Potential Therapeutic Targets for Hepatocellular Carcinoma Using Integrated Bioinformatic Analysis. *Biomed Res Int.* 2019;2019:1245072.
  38. Johnson N, Cai D, Kennedy RD, et al. Cdk1 participates in BRCA1-dependent S phase checkpoint control in response to DNA damage. *Mol Cell.* 2009;35(3):327-339.
  39. Prevo R, Pirovano G, Puliyadi R, et al. CDK1 inhibition sensitizes normal cells to DNA damage in a cell cycle dependent manner. *Cell Cycle.* 2018;17(12):1513-1523.
  40. Perez de Castro I, de Carcer G, Malumbres M. A census of mitotic cancer genes: new insights into tumor cell biology and cancer therapy. *Carcinogenesis.* 2007;28(5):899-912.
  41. Asghar U, Witkiewicz AK, Turner NC, Knudsen ES. The history and future of targeting cyclin-dependent kinases in cancer therapy. *Nat Rev Drug Discov.* 2015;14(2):130-146.
  42. Fang Z, Lin M, Li C, Liu H, Gong C. A comprehensive review of the roles of E2F1 in colon cancer. *Am J Cancer Res.* 2020;10(3):757-768.

## SUPPORTING INFORMATION

Additional supporting information can be found online in the Supporting Information section at the end of this article.

**How to cite this article:** He J, Gao R, Yang J, et al. NCAPD2 promotes breast cancer progression through E2F1 transcriptional regulation of CDK1. *Cancer Sci.* 2023;114:896-907. doi:[10.1111/cas.15347](https://doi.org/10.1111/cas.15347)